THE JOURNAL OF PHYSICAL CHEMISTRY C

Article

pubs.acs.org/JPCC

Energetics of Adsorbed CH_3 and CH on Pt(111) by Calorimetry: Dissociative Adsorption of CH_3I

Eric M. Karp,[†] Trent L. Silbaugh,[†] and Charles T. Campbell*[,†,‡]

[†]Department of Chemical Engineering, University of Washington, Box 351750, Seattle, Washington 98195-1750, United States

[‡]Department of Chemistry, University of Washington, Box 351700, Seattle, Washington 98195-1700, United States

ABSTRACT: The heat of adsorption and sticking probability of methyl iodide were measured on Pt(111) at 95, 215, 270, 300, and 320 K using single crystal adsorption calorimetry (SCAC). On clean Pt(111) at 95 K, the heat of adsorption for molecularly adsorbed methyl iodide was found to be 98.2 ± 2.0 kJ/mol in the limit of low coverage, resulting in a standard enthalpy of formation (ΔH_f^0) of CH_3I_{ad} of −83.6 ± 2.2 kJ/mol. The rate of dissociative adsorption of methyl iodide was fast enough at 320 K for its heat to be accurately measured. The heat of adsorption measured in the low coverage regime (0−0.04 ML) yielded the energetics of adsorbed methyl and iodine adatoms, giving $\Delta H_f^0(CH_{3,ad})$ = −53 kJ/mol (using reported energetics for I_{ad}, which has error bars of ±20 kJ/mol) and a Pt−CH_3 bond strength of 200. kJ/mol. The measured integral heat of adsorption at 0.18 ML and 320 K yielded the energetics of adsorbed methylidyne (CH_{ad}), giving $\Delta H_f^0(CH_{ad})$ between +23 and +42 kJ/mol and a Pt−CH bond strength between 552 and 571 kJ/mol. Using these enthalpies of formation, the enthalpy for the dissociation of adsorbed methane to adsorbed methyl coadsorbed with a hydrogen adatom was found to be +1 kJ/mol, almost thermoneutral. The further reduction of $CH_{3,ad}$ to CH_{ad} + 2 H_{ad} was found to be uphill by between +4 and +23 kJ/mol. Measured methane yields (which require the product H_{ad} from this step) imply that the equilibrium constant for this step lies far to the left, consistent with this reaction's enthalpy. The bond strengths measured here for $CH_{3,ad}$ and CH_{ad} are compared to previous DFT calculations.

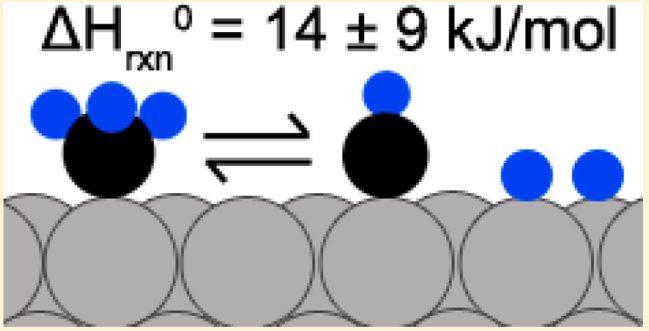

INTRODUCTION

Adsorbed methyl ($CH_{3,ad}$) and methylidyne (CH_{ad}) are known to be key intermediates in energy-related catalysis over late transition metals, including: partial oxidation of methane, steam reforming, combustion and selective oxidations of methane and various other hydrocarbons and oxygenates, methanation, Fischer−Tropsch, methanol decomposition, and several fuel cell reactions. The simple hydrocarbon fragments $CH_{3,ad}$, $CH_{2,ad}$, and CH_{ad} are stable enough to have been identified on both Pt-supported catalysts[1] and Pt(111) single-crystal surfaces at ultrahigh vacuum (UHV) conditions.[2−4] Methyl has been produced on Pt(111) both through dissociative adsorption of methyl iodide[2,5−10] and by azomethane pyrolysis,[11−13] and more recently, $CH_{2,ad}$ and CH_{ad} have been identified on Pt(111) through the dissociative adsorption of CH_2I_2.[3,4] The interactions of CH_3I with Pt(111) have been studied previously in considerable detail.[2,5−10] It is molecularly adsorbed at 100 K

$$CH_3I_g \rightarrow CH_3I_{ad} \quad (1)$$

Some of it desorbs intact during temperature-programmed desorption (TPD) between 170 and 230 K. The rest decomposes to produce $CH_{3,ad}$ plus I_{ad} by 250 K

$$CH_3I_{ad} \rightarrow CH_{3,ad} + I_{ad} \quad (2)$$

At low initial coverage, most of the CH_3I follows this pathway, but at higher coverage, more desorbs. At about the same temperature, the $CH_{3,ad}$ product begins to dehydrogenate and hydrogenate according to the steps

$$CH_{3,ad} \rightarrow CH_{2,ad} + H_{ad} \quad (3)$$

and

$$CH_{3,ad} + H_{ad} \rightarrow CH_{4,g} \quad (4)$$

Reaction 4 is rapid at 250 K since it starts already below 200 K in TPD when $CH_{3,ad}$ + H_{ad} are coadsorbed.[14] While it was initially thought by Zaera et al.[7] that this $CH_{2,ad}$ remained intact at 250 K, later studies in Trenary's group[3] have shown that $CH_{2,ad}$ decomposes already at 130 K via

$$CH_{2,ad} \rightarrow CH_{ad} + H_{ad} \quad (5)$$

and that the CH_{ad} product remains intact up to ∼500 K.[3,4] Thus, any $CH_{2,ad}$ produced in step 3, which occurs at 250−300 K in TPD,[8] must quickly decompose to CH_{ad} + H_{ad}. The fact that CH_{ad} is produced instead of $CH_{2,ad}$ is consistent with stoichiometric ratios measured mass spectroscopically by

Received: January 26, 2013
Revised: February 23, 2013
Published: February 25, 2013

   dx.doi.org/10.1021/jp400902f | J. Phys. Chem. C 2013, 117, 6325−6336

Hendersen et al.[6] and Hugenschmidt et al.[8] Any H_{ad} that is not consumed to make methane desorbs in TPD as $H_{2,g}$ in a broad peak that extends from 270 to 400 K at high coverage.[6−10]

Since the important catalytic parameters of selectivity and activity depend on the thermodynamic stability of adsorbed intermediates, it is important that the energetics (heat of adsorption, bond strength, etc.) of these important adsorbates be measured. Indeed previous studies utilizing temperature-programmed desorption (TPD) have estimated kinetic parameters for methyl conversion to $CH_{4,g}$ and produced estimates for the energetics of adsorbed methyl on Pt(111).[15,16] However, TPD experiments cannot directly measure the adsorption energy of methyl or methylidyne fragments because they do not desorb reversibly from the surface.

Here, we report direct measurements of the standard enthalpies of formation of $CH_{3,ad}$ and CH_{ad} on the Pt(111) surface by calorimetric measurements of the dissociative adsorption of methyl iodide at 270, 300, and 320 K from low to saturation coverages. We already reported the integral heat of adsorption of methyl iodide at one specific condition (0.04 ML and 320 K) which also provided the enthalpy of formation of $CH_{3,ad}$.[17] We show that the measured energetics of adsorbed methyl from SCAC differ from what is reported in previous TPD work[15,16] and further use these values for $CH_{3,ad}$ and CH_{ad} from SCAC to calculate enthalpies of reaction for the stepwise dehydrogenation of methane on Pt(111). These resulting energies will be useful in making predictions about the thermodynamics and activation energies of various catalytically interesting elementary steps over Pt catalysts, and they will also serve as important benchmarks to compare to theoretical calculations (such as density functional theory) to evaluate the energy accuracy of new computational approaches.

EXPERIMENTAL SECTION

Experiments were performed in a UHV chamber (base pressure $<2 \times 10^{-10}$ mbar) equipped with X-ray photoelectron spectroscopy (XPS), Auger electron spectroscopy (AES), low-energy ion scattering spectroscopy (LEIS), low-energy electron diffraction (LEED), and single crystal adsorption calorimetry (SCAC). This apparatus and the procedures for SCAC have been described previously.[18,19]

The sample used was a 1 μm thick Pt(111) single-crystal foil, supplied by Jacques Chevallier at Aarhus University in Denmark. The sample surface was cleaned by 1.25 kV Ar^+ ion sputtering, annealing at 1123 K, then gently heating at 773 K in 1×10^{-8} mbar $O_{2,g}$ for 1 min to remove any surface carbon, and finally flash heating to 1123 K (<1 s). After this treatment, impurities were below the detection limit of AES, and the surface gave a very sharp Pt(111) LEED pattern.

Before calorimetry, the clean Pt(111) sample was brought to thermal equilibrium with the calorimeter and then flash heated to 1123 K (<1 s) to ensure a clean surface. The sample was then brought back into contact with the pyroelectric detector, and thermal equilibrium was re-established (in about 2−5 min), after which the experiment was performed.

Calorimetry was performed by exposing the surface to a pulsed molecular beam of methyl iodide (CH_3I) gas. Each pulse was 100 ms long and repeated every 5 s. The methyl iodide (Fisher Scientific, 99.9%, lot 080482) was outgassed by several freeze−pump−thaw cycles after being put into its reservoir on the vacuum chamber. The reservoir was shielded from light due to methyl iodide's ability to photolyze. Its purity was checked with a mass spectrometer and found to be consistent with the manufacturer's claim. The beam was created by expanding ∼2.0 mbar of CH_3I_g through a microchannel array at 299 ± 6 K (defining the gas temperature) and then collimated through a series of five liquid nitrogen cooled orifices as described previously.[20] Coverages are reported in monolayers (MLs) and are defined as the number of CH_3I molecules that adsorb to the surface irreversibly, normalized by the number of platinum surface atoms in the Pt(111) surface (1.50×10^{19} Pt atoms/m^2). A typical methyl iodide dose was ∼0.004 ML (4.64×10^{12} molecules) per pulse with a beam spot size previously determined to be 4.36 mm in diameter.[20] In a given run, the dose per pulse was highly precise (<1% pulse-to-pulse variation, determined by the reproducibility of the chopper's beam-open time). The absolute accuracy of the measurement of the number of molecules per pulse was better than the measured 3% accuracy of the combined heat measurement, but how much better is difficult to determine. A more detailed description of the experimental principles and implementation of the molecular beam can be found elsewhere.[20,21] The flux of methyl iodide from the molecular beam was measured by impinging the beam onto a liquid nitrogen cooled quartz crystal microbalance (QCM), precovered with multilayers of methyl iodide. Calibration of the QCM has been described previously.[20]

The heat released from the adsorption of one methyl iodide pulse was measured with a pyroelectric polymer ribbon gently pressed against the back side of the Pt(111) sample.[18,22] The sensitivity of the pyroelectric detector was calibrated after each experiment by depositing a known amount of energy into the sample using a HeNe (632.8 nm) laser. The absolute accuracy of the calorimetric heats is estimated to be better than 3% (any systematic errors are less than 3%) for systems like those studied here (i.e., with sticking probabilities above 0.8), based on comparisons to literature values for standard enthalpies of sublimation of the bulk solid when forming solids with known enthalpies.[23] Relative measurements (for example, differences in heat with changes in coverage or temperature) can be much more accurate, and the precision of the energy calibration can be improved as much as desired by averaging multiple runs.

Sticking probabilities were measured simultaneously with calorimetric measurements, using the King and Wells method.[24] A mass spectrometer, without line-of-sight to the sample, measured the background pressure increase of CH_3I_g (m/e = 142) in the chamber. A gold flag was positioned in front of the sample and used to determine the mass spectrometry signal corresponding to full reflection of methyl iodide. The sticking probability of methyl iodide is calculated by integrating the mass spectrometer signal measured from the increase in methyl iodide partial pressure above background when the molecular beam is pulsed onto the sample surface in comparison with the increase in methyl iodide partial pressure resulting when pulsed onto the inert gold flag. We report two types of sticking probabilities, the long-term sticking probability and the short-term sticking probability.[21] The long-term sticking probability, S_∞, is the probability that a gas molecule strikes the Pt(111) surface, sticks, and remains until the next gas pulse starts ∼5 s later. This measurement is used to calculate the adsorbate coverage remaining at the start of the next gas pulse. The short-term sticking probability, $S_{102\ ms}$, is the probability that a gas molecule strikes the Pt(111) surface, sticks, and remains at least throughout the time frame of our heat measurement (i.e., the first 102 ms). This is used to calculate the moles of gas phase reactant that contribute to the

dx.doi.org/10.1021/jp400902f | J. Phys. Chem. C 2013, 117, 6325−6336

measured heat of adsorption, so we can report that value in kiloJoules per mole adsorbed. When there is no desorption between pulses, the two sticking probabilities are the same.

The calorimeter and Pt(111) sample are cooled/warmed by a large thermal reservoir, but one cannot mount a thermocouple directly on the ultrathin single crystal used for calorimetry nor on the sample platen to which it is mounted (because this whole platen is removed from its manipulator and mounted on the thermal reservoir during calorimetry to achieve better signal stability). Therefore, the sample temperature was monitored by two alumel/chromel thermocouples spot-welded to the two closest locations, one spot-welded to the holder of the pyroelectric detector and another to the thermal reservoir. We took the average of these two temperature readings as the sample temperature. For the cryogenic sample temperatures used here (95 and 215 K), the readings of these two thermocouples differed by ∼20 K on average.

RESULTS

Sticking Probability. As described previously[21] and above, we measured two types of sticking probabilities: the long-term sticking probability, S_∞, and the short-term sticking probability, $S_{102\ ms}$. Figure 1 shows both of these sticking probabilities for

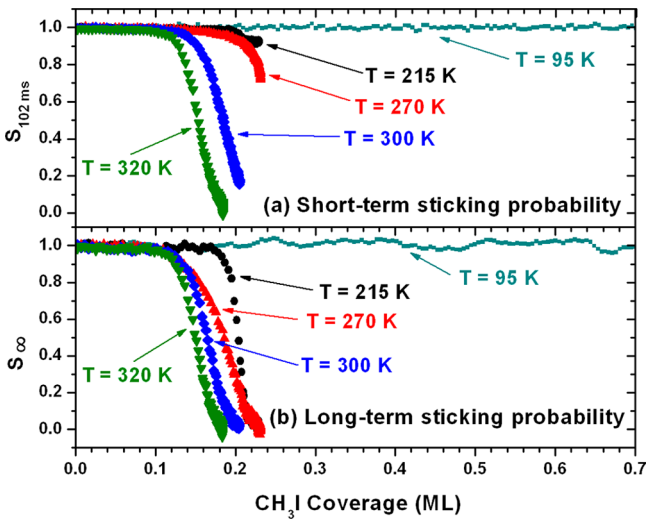

Figure 1. Average short-term (a) and long-term (b) sticking probability of CH_3I on Pt(111) at 95 K (squares), 215 K (circles), 270 K (triangles), 300 K (diamonds), and 320 K (inverted triangles). The long-term sticking probability at 95 K has been smoothed with a 7-point moving average for presentational purposes.

CH_3I_g as a function of coverage on Pt(111) at 95, 215, 270, 300, and 320 K. Even though dissociation is occurring at 270 K and above, the sticking probabilities and coverages in Figure 1 measure the total amount of CH_3I_g that adsorbs to the surface irrespective of the final products produced. At 95 K methyl iodide is known to adsorb molecularly through its iodine atom to the Pt(111) surface[5] in the first layer and at higher coverages form a multilayer. The sticking probabilities measured here (Figure 1) show that a pulse of the methyl iodide completely sticks to the Pt(111) surface for all coverages at 95 K, as seen in both short- and long-term sticking probabilities of 1.00 ± 0.01. This result is consistent with previous TPD studies that found a multilayer to form below ∼112 K.[7−9] At 215 K only the first layer of molecularly adsorbed methyl iodide is stable enough to form since the sample is above the multilayer and second layer desorption peak temperatures of ∼112 and ∼124 K, respectively, but below the first layer desorption peak temperature of ∼225 K.[7−9] At 215 K we find a total saturation coverage for the first layer of 0.23 ML, close to the value of 0.19 ML reported by French and Harrison.[9] Note here the high sticking probability (>0.95) from low coverage up to 0.16 ML, indicating a precursor-mediated adsorption mechanism. This type of adsorption has also been observed for several other organic molecules on Pt(111), namely, benzene,[25] naphthalene,[26] cyclohexene,[21] methanol,[23] and water.[19]

As described above, methyl iodide undergoes C−I bond scission to form adsorbed $CH_{3,ad}$ and I_{ad} on Pt(111) above ∼250 K (reaction 2). The methyl product continues to react by either dehydrogenating to CH_{ad} species (reactions 3 and 5) and/or scavenging adsorbed hydrogen, resulting in the evolution of $CH_{4,g}$ at 260−300 K (reaction 4).[6,7] Thus, these reactions are occurring during our measurements at 270, 300, and 320 K. The saturation coverages here represent the total amount of CH_3I_g that reacted with the surface, irrespective of the products. For these temperatures, the saturation coverage is seen to decrease as the surface temperature increases giving saturation coverages of 0.23, 0.20, and 0.18 ML for Pt(111) at 270, 300, and 320 K, respectively. As shown below, less total methane is produced with increasing temperature between 270 and 320 K, due to a greater probability for methyl dehydrogenation to evolve $H_{2,g}$ rather than to scavenge H_{ad} and evolve methane. We therefore attribute the corresponding decrease in saturation coverage to the decreasing amount of methyl product that escapes the surface as methane and thus whose products remain behind to block sites (see below).

The short-term sticking probability at saturation coverage at 270 K is ∼0.7 and drops to ∼0 when at 320 K. This is because, as the surface temperature increases, the rate constant for desorption of this transiently adsorbed CH_3I_a (on top of the saturated adlayer) increases, and therefore it has a shorter surface residence time. By 320 K, it is so short that it is not long enough to be counted in the short-term sticking probability (which requires a lifetime of at least 102 ms).

Heat of Adsorption at 95 K. In this paper we define the term *heat of adsorption* as the negative of the differential standard molar enthalpy change for the adsorption reaction, with the gas and the Pt(111) being at the same temperature as the Pt(111) surface. During our experiments, the temperature of the molecular beam was ∼300 K, while the Pt(111) sample was held at cryogenic temperatures (e.g., 95 K). Thus, the measured heat is corrected by the small difference in the internal energy of the gas in the *directed* molecular beam at 300 K and in a Boltzmann distribution at the sample temperature (T) and then by RT to convert from internal energy change to enthalpy change for the adsorption reaction, as described elsewhere.[21]

The heat of adsorption of CH_3I_g on Pt(111) at 95 K is shown in Figure 2. At these conditions CH_3I_g adsorbs molecularly through its iodine atom to the Pt(111) surface,[9] initially adsorbing with a heat of 98.2 ± 2.0 kJ/mol. Using the known enthalpy of formation of CH_3I_g[27] and the initial enthalpy of adsorption of methyl iodide on Pt(111) the standard enthalpy of formation of CH_3I_{ad} at 95 K in this low-coverage limit is found to be $\Delta H_f^0(CH_3I_{ad}) = -83.6 \pm 2.2$ kJ/mol. As the coverage increases to 0.25 ML, the heat of adsorption decreases linearly and is well described by a best-fit line of (98.2−110 θ) kJ/mol, where θ is coverage in ML, yielding an average heat of 84 kJ/mol in the first 1/4 ML. The

dx.doi.org/10.1021/jp400902f | J. Phys. Chem. C 2013, 117, 6325−6336

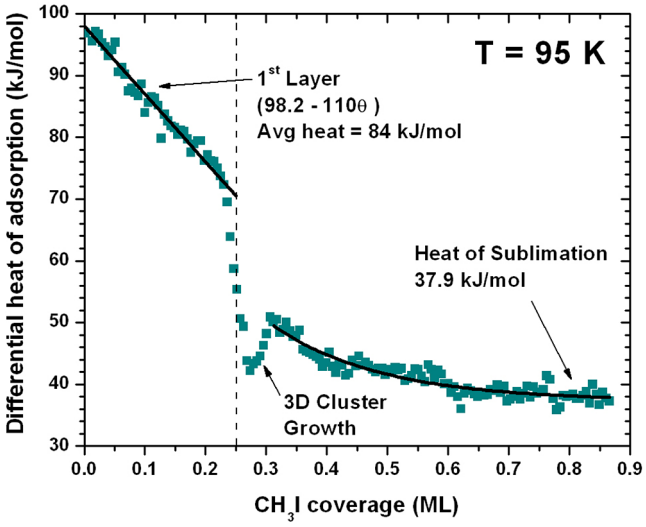

Figure 2. Differential heat of adsorption of CH_3I on Pt(111) at 95 K as a function of coverage. Each data point represents a pulse of 0.004 ML of CH_3I gas and is the result of averaging five experimental runs. At low coverages (θ < 0.25 ML), CH_3I adsorbs molecularly to the Pt(111) surface, and the heat of adsorption exhibits large changes as the coverage increases. At high coverages (θ > 0.65 ML) additional pulses of CH_3I adsorb onto solid CH_3I, and the average heat of adsorption becomes constant at 37.9 ± 2.0 kJ/mol, in agreement with bulk values for the heat of sublimation.

first layer saturation coverage of ~0.25 ML implies only next-to-next nearest-neighbor sites can be occupied in a (2 × 2)-like structure. Following Persson's model,[28] this linear decrease in adsorption energy in the first 1/4 ML can be explained by immobile adsorbates which randomly populate next-to-next nearest-neighbor sites (but not closer) with repulsive interactions between adsorbates at next-to-next nearest-neighbor sites (but not further) and no relaxation of this repulsion by slight movement apart for an isolated pair (i.e., Persson's ε = 0). Adapting Persson's model to a hexagonal lattice, the initial heat of adsorption (98.2 kJ/mol) is the heat of adsorption for a single isolated adsorbate (Persson's μ), and the slope (−110 kJ/mol per ML) is equal to −6 V_0 per 1/4 ML, where V_0 is the pairwise repulsion between adsorbates at next-to-next nearest-neighbor sites (~4.5 kJ/mol here). This is not a surprising result since TPD studies have found the first layer desorption peak temperature to decrease with increasing coverage, indicating repulsive interactions between adsorbates in the first layer.[7,9]

An abrupt ~27 kJ/mol decrease in adsorption enthalpy, down to a value near the bulk heat of sublimation, occurs as the first layer completes at ~0.25 ML, suggesting that additional CH_3I must now adsorb in the much less stable second layer. Then there is an ~10 kJ/mol increase in adsorption energy in the coverage range of 0.26−0.31 ML. This slight increase in stability is likely due to the growth in size of 3D clusters of CH_3I molecules on top of the first layer. That is, more CH_3I−CH_3I bonds are made as the clusters grow in size, thus increasing their stability with increasing coverage, just as we have seen for metal cluster growth on surfaces.[29] Note that just like small 3D clusters of metal atoms these small CH_3I clusters are metastable and will sinter into larger 3D particles in time. Support for this model comes from the reflection absorption infrared spectroscopy (RAIRS) data of French and Harrison[9] that found metastable overlayers of CH_3I forming at low temperatures on Pt(111).

At coverages greater than 0.31 ML, there is a slow exponential decay in the adsorption energy even though the 3D clusters of CH_3I are continuing to grow in size (but probably have already reached the large-size limit energetically). This decay in adsorption energy could be due to a decreasing long-range electronic attraction of the CH_3I adsorbates to the underlying Pt(111) substrate. As the coverage and cluster thickness grow, the average distance between the Pt substrate and newly adsorbed CH_3I molecules increases, and thus the electronic attraction to the Pt diminishes and the heat of adsorption decreases. It asymptotically becomes constant at coverages greater than 0.65 ML at 37.9 ± 2.0 kJ/mol, in excellent agreement with the heat of sublimation of bulk methyl iodide of 38.0 kJ/mol. For the bulk heat of sublimation at 95 K, we used the CH_3I heat of sublimation measured at 207.7 K from ref 30 and corrected it to 95 K by using a gas-phase heat capacity of 4R and the solid heat capacity of CH_3Br, 13 cal/(mol K),[31] since the heat capacity of solid CH_3I is not available.

Reaction Pathways to Adsorbed Methyl and to Methane Evolution. To measure the energetics of adsorbed $CH_{3,ad}$, conditions must be found where the carbon−iodine bond scission (reaction 2) occurs cleanly and fast enough to be detected during the time scale of our heat measurement (~102 ms). The rate constant for this reaction on Pt(111) has been reported in two separate works,[8,9] giving an average value of $k_{rxn} = 9 \times 10^{10}\ s^{-1}\ e^{(-50.8\ kJ/mol/RT)}$. This rate constant is used to estimate the time constant of the carbon−iodine scission ($\tau = 1/k_{rxn}$) as a function of temperature. The resulting τ values show the bond scission occurs with τ = ~100 ms or faster at temperatures of 270 K and above, which is fast enough for the heat to be detected with our measurement. Therefore, experiments conducted at 270 K and above are likely to yield the heat of dissociative methyl iodide adsorption to form adsorbed methyl coadsorbed with iodine (reaction 2). Unfortunately, by 270 K, we also observed the production of methane gas, which shows that we are also producing the further products of reactions 3−5: $CH_{4,g}$, CH_{ad}, and H_{ad}, and possibly $H_{2,g}$.

Figure 3 shows the time dependence of the production rate of methane gas (i.e., its partial pressure) as a single pulse of CH_3I_g is dosed onto the Pt(111) surface at different temperatures. Each pulse of CH_3I_g from the molecular beam lasts 100 ms, consists of approximately 0.0040 ML of CH_3I_g, and is repeated every 5 s. The methane gas signal was measured using a nonline-of-sight mass spectrometer following the signal at m/e = 16. To improve the signal-to-noise ratio here, we averaged all the pulses over the total methyl iodide coverage range from 0.04 to 0.11 ML. No methane gas was evolved in region 1, defined as the range below 0.04 ML.

Figure 4a displays the amount of methane gas evolved from the surface per pulse (i.e., the area under the methane peak in Figure 3) as a function of the total CH_3I_g coverage for different surface temperatures. Figure 4b displays the total integrated amount of methane gas evolved (that is, the sum of all pulse areas, or the integral of Figure 4a) versus total methyl iodide coverage.

As described above, the reaction pathways that are known to be rapid following the adsorption of CH_3I_g on Pt(111) at 270 K can be summarized as reactions 1−5

$$CH_3I_g \rightarrow CH_3I_{ad} \rightarrow CH_{3,ad} + I_{ad} \qquad (1+2)$$

dx.doi.org/10.1021/jp400902f | J. Phys. Chem. C 2013, 117, 6325−6336

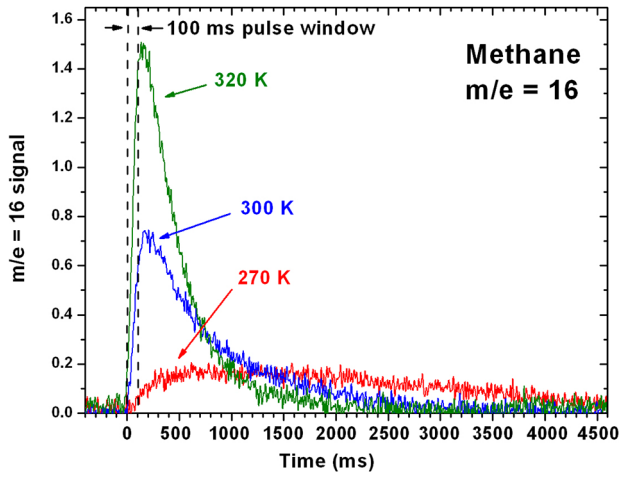

Figure 3. Average line shape of the methane (m/e = 16) mass spectrometer signal for all pulses in the total methyl iodide coverage range from 0.04 to 0.11 ML (region 2) for different temperatures. The dashed lines at 0 and 100 ms define the time window of our heat measurements at 320 K, where the dose of CH_3I begins at 0 ms and ends at 100 ms. Longer heat measurement times are used at 270−300 K (see text).

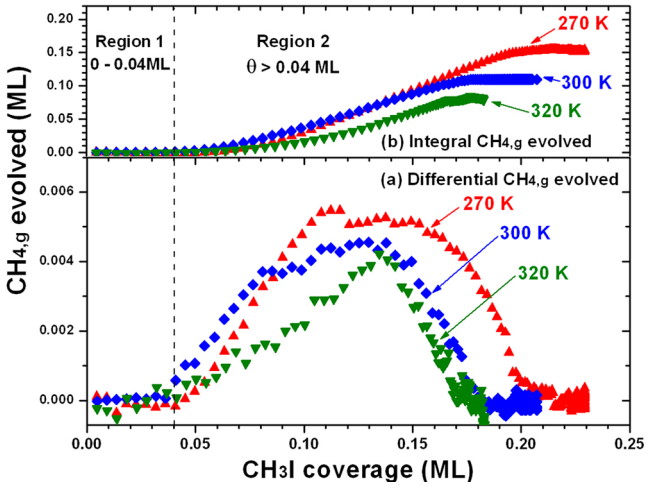

Figure 4. (a) Differential amount of methane gas evolved after each dose of CH_3I_g as a function of coverage for 270, 300, and 320 K. (b) The total integrated amount of methane gas evolved as a function of CH_3I coverage. Two distinct regions are present: region 1 (0 to 0.04 ML) where no methane is evolved and region 2 (>0.04 ML) where methane evolves in increasing and then decreasing amounts.

$$CH_{3,ad} \rightarrow CH_{2,ad} + H_{ad} \rightarrow CH_{ad} + 2H_{ad} \quad (3+5)$$

and

$$CH_{3,ad} + H_{ad} \rightarrow CH_{4,g} \quad (4)$$

If we assume that hydrogen desorption is negligibly slow at 270 K, then these reactions will eventually proceed to completion, giving the net stoichometric reaction

$$3CH_3I_g \rightarrow 2CH_{4,g} + CH_{ad} + 3I_{ad} \quad (6)$$

Thus, for every three methyl iodides, two methanes are produced, and one CH_{ad} remains on the surface with three iodine atoms at completion of the reaction. The saturation coverage of 0.23 ML of reacted methyl iodide (Figure 1b) thus yields (2/3) × 0.23 ML = 0.153 ML of methane, 0.077 ML of CH_{ad}, and 0.23 ML of I_{ad}. Summing these two adsorbates' coverages gives a total saturation coverage of 0.31 ML of all adsorbed species, very close to the value of 1/3 ML expected if only nearest-neighbor sites cannot be occupied by either species. We used this saturation amount of methane at 270 K (0.153 ML) to put ML units on the y axes of Figure 4.

Above 270 K, the saturation coverage decreases (Figure 1b). We attribute this to the fact that a new reaction pathway for H_{ad} (desorption as $H_{2,g}$) gets fast enough to compete with its reaction with $CH_{3,ad}$ to make methane as a mechanism to eliminate H_{ad}. The competition between these two pathways for H_{ad} is shown schematically in Figure 5. As seen in Figure 4b,

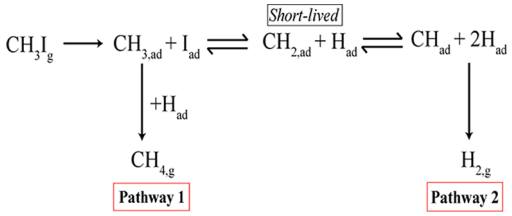

Figure 5. Reaction pathways of CH_3I decomposition on Pt(111), emphasizing the competing pathways by which H_{ad} can be eliminated. Pathway 2 is negligibly slow at 270 K but starts competing with Pathway 1 at 300 K and above. As outlined in the Discussion section, adsorbed methyl is in rapid equilibrium with the CH_{ad} and $2H_{ad}$ species on the right at 270−320 K, but the equilibrium constant for this reaction is very small, so that methyl is heavily favored initially. However, at higher coverages H adatoms are eliminated from the surface via pathways 1 and 2, which forces the equilibrium to the right, ultimately leaving only CH_{ad} and I_{ad} on the surface.

the total amount of methane gas evolved correspondingly decreases to ~0.11 ML at 300 K and ~0.08 ML at 320 K. For each $CH_{3,ad}$ that is not consumed as methane, an additional CH_{ad} remains on the surface. This will thus decrease the saturation amount of reacted methyl iodide by the same amount. These decreases in methane amount (compared to 270 K) by 0.04 ML at 300 K and 0.07 ML at 320 K are close to the decrease in saturation reaction amount in Figure 1b of 0.03 and 0.05 ML, respectively, supporting this explanation for the decrease in saturation coverage with temperature. Subtracting the total methane yield of Figure 4b from the saturation amounts of reacted CH_3I in Figure 1b gives saturation total adsorbate coverages (CH_{ad} + I_{ad}) of 0.29 and 0.28 ML at 300 and 320 K, respectively. Again, these are very close to the value of 1/3 expected if nearest-neighbor sites cannot be occupied.

Figure 4a has two distinct coverage regions: region 1 where no methane is evolved (0 to 0.04 ML) and region 2 (above 0.04 ML) where methane evolves with increasing and then decreasing yields from the surface as successive pulses of CH_3I are dosed. We explain in the Discussion section that the absence of methane in region 1 is due to the equilibrium constant for net reaction 3+5 being very small, so that at low coverage methyl is the dominant C-containing species on the surface; however, as H_{ad} is removed from the surface (by reaction with these methyls, which only occurs fast enough at higher coverages), the reaction is driven to the right, leaving CH_{ad} as the dominant C-containing species by reaction completion. This is consistent with RAIRS results which show that the $CH_{3,ad}$ vibrational modes seen at low temperature disappear after annealing to 300 K and show that modes due to CH_{ad} remain on the surface.[4]

dx.doi.org/10.1021/jp400902f | J. Phys. Chem. C 2013, 117, 6325−6336

Methyl iodide undergoes disproportionation and coupling reactions on Au(111)[32] and β-hydride elimination on Ag(111)[33] and Cu(111),[34] evolving longer chain alkanes/alkenes from the surface. We monitored for these products (ethane, ethylene, propane, propene, butane, and butene), but the only signal observed was methane and its respective cracking pattern, in agreement with previous work.[6,7,9] Hydrogen evolution was also undetected, but this is not unexpected. On the basis of the branching ratios identified above and the stoichiometry of pathway 2 (Figure 5), the amount of hydrogen released even at 320 K would be below our detection limits given the background signal of $m/e = 2$ in the chamber and the mass spectrometer's sensitivity to $H_{2,g}$.

At 270 K, the $m/e = 16$ line shape in Figure 3 shows that the $CH_{4,g}$ signal continues to rise long after the 102 ms time window typically used for the heat measurement (between the two dashed lines in Figure 3). This situation should result in a line shape change in the heat detector signal,[19] as indeed observed (see below). The same is true at 300 K, but to a lesser extent. In both cases, this leads to a broadening in the heat signal, which is more complicated to interpret quantitatively to extract heats, as described below. However, by 320 K, methane is evolved in region 2 sufficiently fast to reach a maximum at the end of the pulse window in Figure 4, meaning the signal from the heat detector at 320 K in region 2 should exhibit little to no broadening and accurately represent the chemistry occurring here.

Heat of Adsorption of Methyl Iodide on Pt(111) at 215, 270, 300, and 320 K. Figure 6 displays the heat of adsorption versus coverage for methyl iodide dosed onto Pt(111) at 215, 270, 300, and 320 K.

At 215 K the average heat of adsorption is 96.4 kJ/mol, 11 kJ/mol larger than the average heat of adsorption measured at 95 K in the same coverage range (0–0.23 ML, Figure 2). Using a mass spectrometer positioned normal to the Pt(111) surface, Harrison and French[9] observed small amounts of methane evolution at this temperature, indicating a small amount of decomposition of CH_3I_{ad} that could contribute to this higher heat. We did not observe any methane evolution, but because our mass spectrometer is not normal to the surface it is unlikely that our measurement is as sensitive. However, the rate constant equation listed above gives a reaction time constant of 24 s for the carbon–iodine bond scission at this temperature, which is much too slow to be detected during our ~100 ms heat detection window. Therefore the 11 kJ/mol higher heat at 215 K is likely the result of adsorbed CH_3I molecules in a more stable phase at 215 K than at 95 K. This could be due to the fact that the greater mobility at higher temperature allows the molecules to arrange into their most stable structure on the time scale of the heat measurement at 215 K, but not at 95 K.

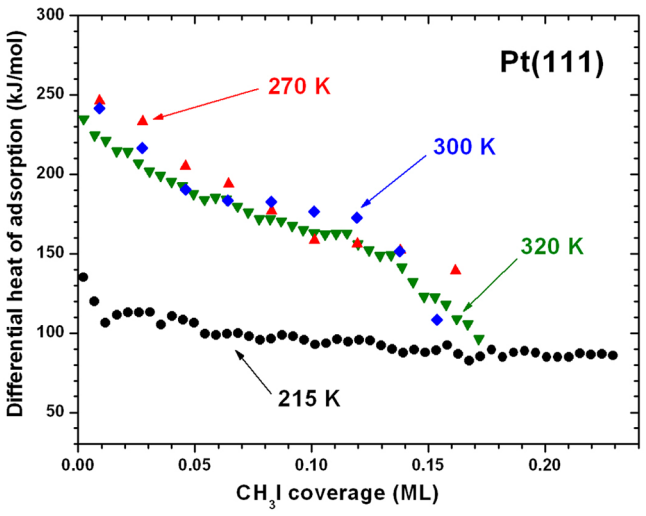

Figure 6. Differential heat of adsorption of CH_3I on Pt(111) versus coverage in the temperature range 215–320 K. The data points at 215 and 320 K represent a pulse of ~0.004 ML of CH_3I gas and are the results of averaging five experimental runs. As described in the text, the data at 270 and 300 K have been corrected for a broadened line shape that resulted from slow reaction kinetics depositing heat on a time scale longer than the window of the molecular beam pulse.

The heat signal pulses at 270 K showed significant broadening compared to that from the laser calibration signal, consistent with the slow evolution of methane seen in Figure 3. Such pulse broadening is due to a surface reaction depositing heat on a time scale slightly longer than the 100 ms pulse width of the molecular beam, as discussed previously in detail elsewhere,[19] where we showed an example of how the line shape broadens. Interpretation of the broadened heat signal is complicated since the observed signal is really a convolution of sequential heat events. In region 1, the lack of methane evolution (Figure 4a) coupled with previous RAIRS studies showing high concentrations of $CH_{3,ad}$ species[3,4,7,9] leads to the following model of sequential reaction events that contribute to the heat

$$CH_3I_g \rightarrow CH_3I_{ad} \quad (1)$$

$$CH_3I_{ad} \rightarrow CH_{3,ad} + I_{ad} \quad (2)$$

We assumed that step 1 is instantaneous at 270 K and above (as is usually the case for such simple molecular adsorption events) and that reaction 2 proceeds with a pseudofirst-order rate constant $k_2 = 1/\tau$, thus giving rise to an exponential decay function with time constant τ which is convoluted with the reactant input from step 1, which was set equal to the molecular beam pulse shape. The heats from both steps are also convoluted with the calorimeter's instrument response function (measured by its response to the laser pulses used for signal calibration). We were able to deconvolute our observed heat signal into these two heat components by constructing theoretical signals for each heat event and summing them together until a best fit of the measured signal was obtained. The heat of step 1, the heat of step 2, and the time delay, τ, of step 2 were all adjusted until the resulting modeled signal (i.e., the sum of these two simulated signals) converged to fit the measured signal. This analysis provides the differential heat of steps 1 and 2, the total differential heat of the reaction, and the rate constant for step 2 where $k_2 = 1/\tau$. We are preparing a separate manuscript to describe the details of this and other new methods we have developed for analyzing broadened heat signals in SCAC.

At higher coverages, reactions 3–5 also proceed, eventually giving net reaction 6. We assume here that steps 2–5 can be described by a single, pseudofirst-order rate constant, so that at higher coverages this same deconvolution analysis provides the heat for step 1, the total differential heat of the more complicated net reaction that is occurring at each coverage, and the pseudofirst-order rate constant, $1/\tau$. As shown below, this pseudofirst-order analysis works well, probably because the latter steps are fast and rate limited by step 2.

dx.doi.org/10.1021/jp400902f | J. Phys. Chem. C 2013, 117, 6325–6336

For the data at 270 K we found that τ increased linearly with coverage from ~170 ms initially to 750 ms at 0.23 ML. This corresponds to a decrease in k_2 from 5.9 to 1.3 s^{-1}. The reason k_2 decreases with coverage may be that as more active sites become blocked by adsorbates the pseudofirst-order rate constant decreases as expected if it is really the product of a true second-order rate constant and the free site concentration. Lateral interactions with coadsorbates might also affect the activation energy for step 2. At 300 K, τ increased with coverage from ~70 to ~250 ms. At both 270 and 320 K, the mechanism is more complex than just reactions 1 plus 2, as discussed below.

At 320 K the kinetics were fast enough that no broadening of the heat signal line shape was detected, consistent with the methane evolution rate in region 2 at 320 K being fast enough to occur in the time frame of the heat measurement (Figure 3). In Figure 6, the heat versus coverage curves for the corrected data at 270 and 300 K approximately follow the heat curve measured at 320 K, confirming that similar heats are measured at these temperatures, but with slower kinetics at 270 and 300 K. As discussed previously,[35] it is most reliable to perform SCAC at conditions where the reaction is fast enough to occur within the 100 ms pulse of the molecular beam, so that no deconvolution is needed.[19] Therefore, the 320 K heat curve in Figure 6 is assumed to be the most accurate in representing the heat released during the surface reactions. At 270 and 300 K, the data interpretation in region 2 is also complicated by the fact that most of the methane is evolved more slowly than the heat signal time constant τ.

DISCUSSION

Energetics of Adsorbed Methyl on Pt(111). The lack of methane evolution in region 1 (0−0.04 ML) in Figure 4a indicates that reactions 3−5 are not yet occurring. We show below that this is not because they are too slow at 270−320 K but instead because their net equilibrium lies far to the left. We thus take the heat in region 1 at 320 K (Figure 6) to represent the net heat of steps 1 plus 2 above, or net reaction 1+2. The measured integral heat of adsorption in this coverage range (212 kJ/mol) gives the enthalpy of net reaction 1+2 to be −212 kJ/mol. A thermodynamic cycle was constructed in our earlier report[17] to extract from this the standard enthalpy of formation (ΔH_f^0) and Pt−C bond enthalpy for adsorbed methyl. We found ΔH_f^0 ($CH_{3,ad}$) to be −53 kJ/mol, which is the total enthalpy change in taking the elements in their standard states to adsorbed methyl on Pt(111), and the H_3C−Pt(111) bond enthalpy is 200. kJ/mol. This used the enthalpy of formation of I_{ad} on Pt(111), which is known to be −144 kJ/mol at 0.04 ML from the TPD work of Labayen et al.[36] The maximum potential error in these numbers was estimated to be ±20 kJ/mol, based on the dominant error of ±20 kJ/mol on the heat of formation of I_{ad} from TPD.[36] The coadsorption of iodine at such low coverage should not affect these numbers significantly.[17]

Energetics of Adsorbed Methylidyne on Pt(111). As noted above, the net reaction at 270 K at reaction completion is:

$$CH_3I_g \rightarrow 2/3CH_{4,g} + 1/3CH_{ad} + I_{ad} \quad (7)$$

Thus, the integral heat of adsorption at saturation coverage at 270 K should give the heat for this net reaction. The net methane yield is 2/3 of the saturation amount of reacted CH_3I (0.23 ML), or 0.153 ML. At 300 K, the methane yield decreased to 0.11 ML (Figure 4b) since some of the H_{ad} that is used to produce methane in reaction 6 instead desorbed as $H_{2,g}$, and the saturation coverage also decreased to only 0.20 ML. This gives the following net reaction at completion at 300 K

300 K:

$$CH_3I_g \rightarrow 0.55CH_{4,g} + 0.45CH_{ad} + 0.175H_{2,g} + I_{ad} \quad (8)$$

Similarly, only 0.08 ML of methane was produced at 320 K (Figure 4b), and the saturation coverage decreased to 0.18 ML. This gives the following net stoichiometry at reaction completion and 320 K

320 K:

$$CH_3I_g \rightarrow 0.44CH_{4,g} + 0.56CH_{ad} + 0.34H_{2,g} + I_{ad} \quad (9)$$

We have analyzed our integral heats of adsorption at these temperatures assuming these stoichiometries, with two corrections: The rate of hydrogen desorption is so slow compared to the heat measurement time τ that the H_{ad} has not yet converted to gas. (Using the reported prefactor and activation energy for hydrogen desorption from Pt(111)[37] gives much longer surface residence times.) Thus, we replace every $H_{2,g}$ with 2 H_{ad} for the purposes of analyzing reaction heats. Similarly, most of the methane is evolved after the heat measurement time τ at 270 and 300 K, so that we must replace $CH_{4,g}$ with $CH_{3,ad}$ + H_{ad} there too.

Unfortunately, the heat curves in Figure 6 do not extend all the way up to the saturation coverages of Figure 1; however, the heat curve comes very close at 320 K, and it decreases linearly with coverage at the highest coverages measured. Thus, we assumed that this decrease continues linearly at 320 K up to saturation coverage. This gives a final heat of adsorption of 89 kJ/mol at 320 K. We then assumed that this final heat of adsorption of 89 kJ/mol was the same at 300 and 270 K and connected the point in Figure 6 for last heat value to this saturation coverage point assuming a straight-line decrease. We then used the integrals of these (analytically continued) heat curves to calculate the integral heats of adsorption. These values are tabulated in Table 1 versus temperature.

Using the total integral heats measured at each temperature from Table 1 together with the reaction stoichiometries outlined above, we calculate the standard enthalpy of formation of CH_{ad}, ΔH_f^0 (CH_{ad}), at each temperature. This calculation required the standard enthalpy of formation of all the other reactants and products in these reactions. For adsorbed iodine, we used the coverage-dependent heat of formation: a value of −125 kJ/mol at 0.23 ML of I_{ad} for the reaction at 270 K, −128 kJ/mol at 0.20 ML I_{ad} for 300 K, and −130 kJ/mol at 0.18 ML I_{ad} for 320 K. These coverage-dependent heats of formation of iodine adatoms are found from the reported heat of adsorption of iodine extracted from careful analysis of TPD data.[36] We also used here the reported enthalpy of adsorption of $H_{2,g}$ at low coverage (−72 kJ/mol)[21] for the standard heat of formation of $2H_{ad}$. Since methane is known to be produced by reaction 4 with 18.7 kJ/mol of excess enthalpy (above that expected for a Boltzmann distribution at the surface temperature),[38] we corrected its standard heat of formation taken from the literature (−75 kJ/mol[39]) by this amount. For CH_3I_g, the standard heat of formation is +14.6 kJ/mol.[27]

Also listed in Table 1 is the HC−Pt(111) bond enthalpy for CH_{ad}, calculated at each temperature by subtracting ΔH_f^0(CH_{ad}) from the standard enthalpy of formation of CH_g (594 kJ/mol[39]).

dx.doi.org/10.1021/jp400902f | J. Phys. Chem. C 2013, 117, 6325−6336

Table 1. Integral Heats of CH_3I Adsorption for Saturation Coverage at Different Temperatures and Their Corresponding Reaction Stoichiometries, Along with the Values for $\Delta H_f^0(CH_{ad})$ and the Pt−CH Bond Enthalpy Determined from These[a]

temp (K)	overall reaction	final coverages (ML) θ_{CH}	final coverages (ML) θ_I	integral enthalpy of adsorption (kJ/mol)	no destabilization of coadsorbates $\Delta H_f^0(CH_{ad})$ (kJ/mol)	no destabilization of coadsorbates Pt−CH bond enthalpy (kJ/mol)	$CH_{3,ad}$ destabilized by 30 kJ/mol $\Delta H_f^0(CH_{ad})$ (kJ/mol)	$CH_{3,ad}$ destabilized by 30 kJ/mol Pt−CH bond enthalpy (kJ/mol)	H_{ad} destabilized also by 15 kJ/mol $\Delta H_f^0(CH_{ad})$ (kJ/mol)	H_{ad} destabilized also by 15 kJ/mol Pt−CH bond enthalpy (kJ/mol)
270 K	$CH_3I_g \rightarrow 2/3(CH_{3,ad} + H_{ad}) + 1/3CH_{ad} + I_{ad}$	0.077	0.23	−163	+109	485	+48	546	+18	576
300 K	$CH_3I_g \rightarrow 0.55(CH_{3,ad} + H_{ad}) + 0.45CH_{ad} + 0.35H_{ad} + I_{ad}$	0.090	0.20	−167	+83	511	+46	548	+16	578
320 K	$CH_3I_g \rightarrow 0.44CH_{4,g} + 0.56CH_{ad} + 0.68H_{ad} + I_{ad}$	0.11	0.18	−171	+42	552	+42	552	+23	571

[a]The values under the label "No Destabilization of Coadsorbates" use the heats of formation for CH_{ad} and H_{ad} measured at very low coverages. The other columns instead assume that these heats of formation are higher by 30 and 15 kJ/mol, respectively, due to adsorbate−adsorbate repulsions.

As seen in Table 1, under the heading "no destabilization of coadsorbates", the results at these three temperatures give different heats of formation for CH_{ad}: +109 kJ/mol at 270 K, +83 kJ/mol at 300 K, and +42 kJ/mol at 320 K. The differences could be due to an inaccurate value of $\Delta H_f^0(CH_{3,ad})$ used for the 270 and 300 K data. We used here the value measured at very low coverage (−53 kJ/mol at 0.04 ML, see above) but applied it over the full coverage range up to saturation (i.e., coadsorbed with 0.20−0.23 ML of I_{ad}). At such high coverages, $CH_{3,ad}$ is probably substantially less stable due to adsorbate−adsorbate repulsions. To investigate this effect, we instead assumed that the stability of $CH_{3,ad}$ is lowered by 30 kJ/mol (i.e., $\Delta H_f^0(CH_{3,ad}) = -23$ kJ/mol) at these high-coverage conditions, as shown under the heading "$CH_{3,ad}$ destabilized by 30 kJ/mol". This brings the values for CH_{ad} at 270 and 300 K to within 6 kJ/mol of the value at 320 K (where no correction is needed since no $CH_{3,ad}$ is produced). We similarly investigated the effect of destabilization of H_{ad} at these high coverages by decreasing the heat of adsorption of $H_{2,g}$ by 30 kJ/mol (i.e., $\Delta H_f^0(H_{ad}) = -21$ kJ/mol). This increased the stability of CH_{ad} and the Pt(111)−CH bond energy by an additional 30 kJ/mol at these temperatures and by 19 kJ/mol at 320 K. The combined effect of destabilizing CH_{ad} and H_{ad} is to decrease the $\Delta H_f^0(CH_{ad})$ to +19 ± 4 kJ/mol and increase the HC−Pt(111) bond enthalpy to 575 ± 4 kJ/mol at all three temperatures. However, for the reasons mentioned above, the values at 320 K, which are at the lower-stability end of this range, are assumed to be the most accurate since they require fewer approximations.

Therefore, our most accurate heat measurement at 320 K in Table 1 give a range of Pt−CH bond energies between 552 and 571 kJ/mol. This result can be compared to a calorimetry experiment by Yeo et al. for ethylidyne ($-CCH_3$) on Pt(111),[40] which should have a similar bond energy as −CH. In that work, Yeo et al. reported a bond energy for ethylidyne to Pt(111) of 675−684 kJ/mol (or 225−228 kJ/mol per Pt−C bond). However, we recently reported that this group had a calibration error in their calorimetry results on Pt(111) due to an incorrect reflectivity value for Pt(111).[41] Correcting for this error just as we suggested there[41] gives a corrected bond energy for ethylidyne of ∼633 kJ/mol. The value we measured here for −CH is still ∼71 kJ/mol smaller than that for ethylidyne. However, our values are for CH coadsorbed with iodine at saturation coverage, whereas the value for ethylidyne was in the limit of low coverage; so, this difference is probably mainly due to repulsive interactions between CH_{ad} and coadsorbed CH_{ad} and I_{ad}.

It is rather surprising that the adsorption of methyl iodide initially produces mainly $CH_{3,ad}$ (plus I_{ad}) at low coverages for all three of these temperatures, but at high coverages the only surface product remaining is CH_{ad} (plus I_{ad}). We next prove that this is a natural consequence of the very small equilibrium constant for net reaction 3+5

$$CH_{3,ad} \rightleftharpoons CH_{ad} + 2H_{ad} \qquad (3+5)$$

At low coverage methyl is the dominant C-containing species on the surface, but as H is removed from the surface (by reaction with these methyls to make methane gas, which only occurs fast enough at higher coverages), the reaction is driven to the right, so that CH_{ad} is the dominant C-containing species by reaction completion. This push to the right is an example of Le Chatelier's Principle.

dx.doi.org/10.1021/jp400902f | J. Phys. Chem. C 2013, 117, 6325−6336

In Figure 7 we show the coverages of $CH_{3,ad}$, CH_{ad}, and H_{ad} versus methyl iodide coverage calculated to simulate the exact

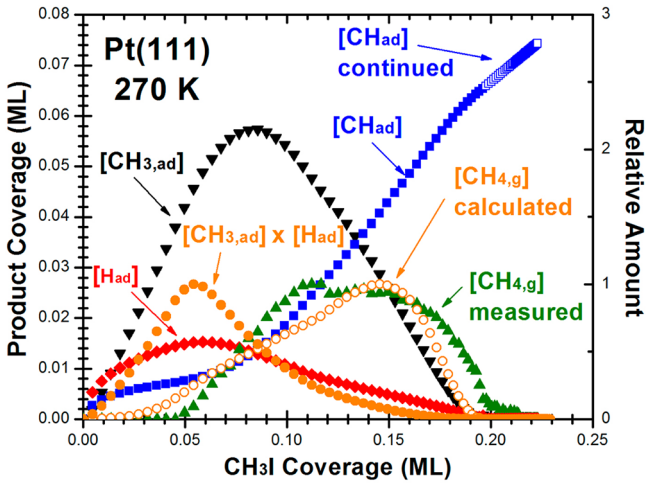

Figure 7. Calculated coverages of $CH_{3,ad}$, H_{ad}, and CH_{ad} on Pt(111) at 270 K versus the amount of CH_3I that adsorbed, assuming an equilibrium constant of 4×10^{-5} for reaction 3+5 and using the measured amount of methane evolved (also shown). Shown here is the product $[CH_3][H]$ and the rate of CH_4 evolution calculated from this product assuming that the rate constant k_4 has an activation energy that decreases linearly by 19 kJ/mol as coverage increases across this plot. Above the methyl iodide coverage where the methyl coverage drops to nearly zero (0.19 ML), the measured amounts of methane evolved, and methyl iodide adsorbed became so small compared to the noise that the calculation of coverages became mathematically degenerate. However, since there is no more methyl to consume at these higher coverages, we know that the net stoichiometry at each pulse must be that given by reaction 6, so we analytically continued the coverage of CH_{ad} above there by assuming a slope of 1/3 as predicted by this stoichiometry (open squares).

conditions of our calorimetry experiment at 270 K. These coverages were calculated by incrementally changing the adsorbate coverages with each methyl iodide gas pulse (starting from zero initially) based on the following simple model:

1. The methyl coverage was first increased by the measured amount of methyl iodide that adsorbed in that pulse period (i.e., its flux times and its long-term sticking probability).

2. The coverages of $CH_{3,ad}$ and H_{ad} were each decreased by the measured amount of methane gas evolved during that pulse period (also plotted in Figure 7).

3. The net reaction 3+5 was then assumed to come to equilibrium with an equilibrium constant

$$K_{3+5} = ([CH][H]^2)/[CH_3] = 4 \times 10^{-5}\ ML^2$$

where [i] represents the surface coverage of species i in ML. This value for K_{3+5} was estimated from our measured enthalpy of reaction 3+5 of +23 kJ/mol estimated from the 320 K data (see below), neglecting any estimated destabilization of $CH_{3,ad}$ and H_{ad} by coadsorbates and also neglecting any entropy difference between reactants and products, so that $K_{3+5} = \exp[(-23\ kJ/mol)/RT]$. The final equilibrium coverages of $CH_{3,ad}$, CH_{ad}, and H_{ad} at the end of the pulse period were calculated based on their initial values (i.e., after step 2) and this equilibrium constant. Steps 1−3 were repeated for each gas pulse.

As seen in Figure 7, this simple model leads to the following interesting and nonintuitive results. Initially, almost 100% of the MeI that adsorbs is used to build up the coverage of $CH_{3,ad}$ below 0.06 ML; however, above 0.09 ML, that $CH_{3,ad}$ is removed almost as rapidly and there is a similar rapid buildup in the coverage of CH_{ad}. This transition occurs when the amount of methane gas evolved per pulse gets large. This trend continues until essentially all the $CH_{3,ad}$ is consumed, and the methane gas evolution also drops to near zero.

The slopes of +0.56 for CH_{ad} and −0.66 for $CH_{3,ad}$ in the coverage range 0.11−0.17 ML in Figure 7 are close to the values of 1/2 and −1/2 expected for the following net stoichiometry: $2CH_3I_g + CH_{3,ad} \rightarrow CH_{ad} + 2CH_{4,g} + 2I_{ad}$. However, there seems to be some small contribution from the following stoichiometry as well: $CH_3I_g + 2CH_{3,ad} \rightarrow CH_{ad} + 2CH_{4,g} + I_{ad}$, which would give larger slopes of +1 and −2 if occurring alone.

It is also surprising that methane gas does not appear already at lower coverage. We next show that this is a natural consequence of the kinetics of reaction 4 that produces methane from surface methyl plus H, provided that its activation energy decreases linearly with coverage by a small amount. The rate of reaction 4 should be proportional to the product $[CH_3][H]$ and a rate constant, k_4. In Figure 7, we plot also the product $[CH_3][H]$. It maximizes at a much lower coverage than the measured methane evolution rate (amount per pulse). However, if we assume that k_4 has an activation energy that decreases with coverage by 94 kJ/mol per ML of MeI, we instead get the calculated rate of CH_4 production shown in Figure 7. This maximizes at much higher coverage and semiquantitatively reproduces the coverage dependence of the measured rate. This decrease in activation energy by 94 kJ/mol per ML of MeI corresponds to only 19 kJ/mol for the whole coverage range plotted here. This small amount is entirely reasonable, given the fact that both reactants ($CH_{3,ad}$ and H_{ad}) are certainly greatly destabilized relative to the product as coverage increases, due to adsorbate−adsorbate repulsions.

Predicted Reaction Enthalpies. The standard enthalpies of formation of adsorbed methyl (−53 kJ/mol) and methylidyne (between +23 and +42 kJ/mol) measured in this work on Pt(111), along with literature values for ΔH_f^0 of $CH_{4,g}$ (−75 kJ/mol[39]) and H_{ad} (−36 kJ/mol at low coverage[21]), allow the following reaction enthalpies of methane dehydrogenation steps on Pt(111) to be calculated

$$CH_{4,g} \rightarrow CH_{3,ad} + H_{ad} \quad \Delta H^0_{rxn10} = -14\ kJ/mol \qquad (10)$$

$$CH_{4,ad} \rightarrow CH_{3,ad} + H_{ad} \quad \Delta H^0_{rxn11} = +1\ kJ/mol \qquad (11)$$

$$CH_{3,ad} \rightarrow CH_{ad} + 2H_{ad} \quad \Delta H^0_{rxn12} = +4\ to\ +23\ kJ/mol \qquad (12)$$

For reaction 11, we used $\Delta H_f^0(CH_{4,ad}) = -90.1$ kJ/mol, which is calculated from the $\Delta H_f^0(CH_{4,g}) = -75$ kJ/mol[39] and the desorption energy of methane from Pt(111) (15 kJ/mol, measured by TPD[42]). The energetics of reactions 10−12 are summarized in Figure 8. The energy of $CH_{2,ad}$ is not known but is only shown as less stable than $CH_{ad} + H_{ad}$ since it decomposes into these products already at 130 K.[3,4]

Comparison to DFT. The reaction enthalpies measured in this work provide benchmarks for comparison to DFT calculations of methyl and methylidyne on Pt(111). The enthalpy of reaction 11, $CH_{4,ad} \rightarrow CH_{3,ad} + H_{ad}$, is +1 kJ/mol, nearly thermoneutral. DFT calculations utilizing the PW91 functional find a similar enthalpy of −7.7 kJ/mol.[43] The

dx.doi.org/10.1021/jp400902f | J. Phys. Chem. C 2013, 117, 6325−6336

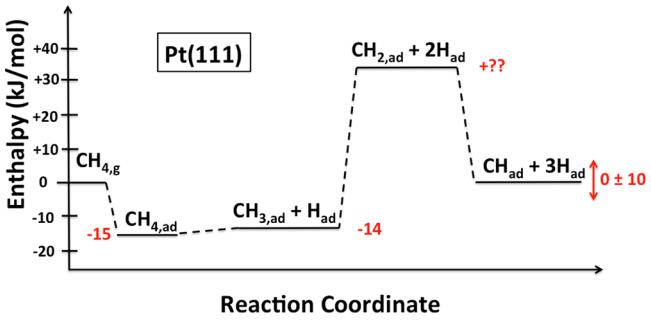

Figure 8. Reaction enthalpy landscape for three steps of methane dehydrogenation on Pt(111) calculated from the heats of formation of methyl fragments measured in this work and referenced to methane gas. The enthalpy change taking methane gas to adsorbed methyl plus a hydrogen adatom is downhill in energy by 14 kJ/mol. The deeper dehrydrogenation of methane gas to CH_{ad} + $3H_{ad}$ is found to be between −10 and +9 kJ/mol. Note here that the enthalpy for dehydrogenation of methane gas to $CH_{2,ad}$ and two hydrogen adatoms is unknown but is shown here higher than CH_{ad} + $3H_{ad}$ since $CH_{2,ad}$ is known to decompose at low temperatures (∼130 K) to CH_{ad} + H_{ad}.

enthalpy for reaction 12 is between +4 and +23 kJ/mol, which is different than the reaction energy of −38 kJ/mol calculated by DFT.[43] Summing the enthalpies for reactions 11 and 12 gives a total enthalpy between +5 and +24 kJ/mol for $CH_{4,ad}$ → CH_{ad} + $3H_{ad}$, whereas DFT calculates this reaction enthalpy to be −45 kJ/mol.[43]

Table 2 lists calculated bond energies for these adsorbates to Pt(111) using cluster and periodic-boundary DFT calculations and compares them to our measurements. The bond energies of $CH_{3,ad}$ and CH_{ad} listed in Table 2 were found by subtracting RT from the bond enthalpies.

Table 2. Bond Energies of Methyl and Methylidyne to the Pt(111) Surface Reported from Previous DFT Calculations and Compared to the Present Measurements[a]

species	functional	coverage or cluster size	bond energy (kJ/mol)	reference
$CH_{3,ad}$ (atop)	current experiment	0.04 ML with 0.04 ML I_{ad}	197	this paper
	B3LYP	35 atom cluster	209	44
	B3LYP	10 Pt atom cluster	209	45
	PW91	10 Pt atom cluster	232	45
	B3LYP	8 Pt atom cluster	225	46
	PW91	1/4 ML	197	47
	RPBE	1/4 ML	163	47
	PBE	1/9 ML	192	48
CH_{ad} (fcc hollow)	current experiment	saturation CH_3I dose at 320 K	549−568	this paper
	B3LYP	35 Pt atom cluster	613	44
	B3LYP	10 Pt atom cluster	678	45
	PW91	10 Pt atom cluster	728	45
	B3LYP	8 Pt atom cluster	697	46
	PW91	1/4 ML	620	47
	RPBE	1/4 ML	569	47
	PBE	1/9 ML	643	48

[a]This comparison to DFT for $CH_{3,ad}$ has already been reported[17] and is included here so that the accuracies of the same DFT methods can also be compared for these two different species.

Caution must be used when comparing the measured bond energy of methylidyne from this work to DFT calculations because the HC−Pt(111) bond energy measured here is for a saturation coverage of −CH coadsorbed with ∼0.18−0.23 ML of I_{ad}, where adsorbate−adsorbate repulsions are likely to destabilize the CH_{ad}. While it is known that coadsorption with a small coverage of I_{ad} does not significantly affect $CH_{3,ad}$ groups, at least in their reaction rates as measured by TPD,[2] it is expected that iodine adatoms perturb neighboring methylidyne adsorbates when at these high saturation coverages.

CONCLUSIONS

Single-crystal adsorption calorimetry of methyl iodide adsorption on Pt(111) at 95, 270, 300, and 320 K has yielded the energetics of molecularly adsorbed methyl iodide, adsorbed methyl, and adsorbed methylidyne.

At 95 K, methyl iodide adsorbs to Pt(111) molecularly through its iodine atom, forming a (2 × 2)-like structure with repulsive dipole−dipole interactions between adsorbates resulting in a decreasing heat of adsorption that is well fit by (98.2−110 θ) kJ/mol up to 0.25 ML of coverage. These results give a $\Delta H_f^0(CH_3I_{,ad})$ = −83.6 ± 2.2 kJ/mol for adsorbed methyl iodide in the limit of low coverage. Above 0.25 ML, methyl iodide adsorbs in a second layer structure forming 3D clusters of CH_3I that increase in stability as their size grows with coverage. At coverages greater than 0.6 ML methyl iodide adsorbs with a constant heat of adsorption equal to the heat of sublimation of methyl iodide. At 215 K, only the first 0.23 ML of methyl iodide adsorbs, with an integral heat of molecular adsorption that is 11 kJ/mol higher than at 100 K in this same coverage range.

At temperatures of 270−320 K, methyl iodide dissociatively adsorbs, forming $CH_{3,ad}$ coadsorbed with iodine adatoms in the coverage range 0−0.04 ML. Heat measurement in this coverage region gave $\Delta H_f^0(CH_{3,ad})$ = −53 kJ/mol and a Pt−CH_3 bond enthalpy of 200. As the coverage increases past 0.04 ML, dehydrogenation of these methyl groups results in the formation of methane and H_2 gas, which ultimately leaves CH_{ad} coadsorbed with iodine adatoms. The kinetics of these reactions are fast enough at 320 K to accurately measure the reaction heats with SCAC. The integral heat measurements from 0 ML to saturation coverage at 270, 300, and 320 K provided the energetics of adsorbed methylidyne, giving $\Delta H_f^0(CH_{ad})$ between +23 and +42 kJ/mol and a Pt−CH bond enthalpy between 552 and 571 kJ/mol at 320 K. From the measured enthalpies of formation of adsorbed methyl and methylidyne, the enthalpy of methane dehydrogenation steps on Pt(111) was calculated, giving an enthalpy for $CH_{4,ad}$ → $CH_{3,ad}$ + H_{ad} of +1 kJ/mol, almost thermoneutral, and an enthalpy for $CH_{3,ad}$ → CH_{ad} + 2 H_{ad} between +4 and +23 kJ/mol.

The measured bond enthalpies of Pt−CH_3 and Pt−CH were compared to previous DFT calculations. Cluster calculations were found to routinely overestimate the bond strength of both $CH_{3,ad}$ and CH_{ad} but move closer to the measured value as cluster size increases. Periodic DFT calculations performed better, with the level of agreement depending on the functional.

AUTHOR INFORMATION

Corresponding Author

*E-mail: campbell@chem.washington.edu.

Notes

The authors declare no competing financial interest.

■ ACKNOWLEDGMENTS

The authors acknowledge support for this work by the National Science Foundation under CHE-CHE-1010287. We also wish to acknowledge John W. Heutink and Brian P. Holm at the Chemistry Department machine shop for their invaluable skill and expertise.

■ REFERENCES

(1) McGee, K. C.; Driessen, M. D.; Grassian, V. H. Infrared Study of the Adsorption and Reaction of Methyl Chloride and Methyl Iodide on Silica-Supported Pt Catalysts. *J. Catal.* **1996**, *159*, 69−82.
(2) Zaera, F. Preparation and Reactivity of Alkyl Groups Adsorbed on Metal Surfaces. *Acc. Chem. Res.* **1992**, *25*, 260−265.
(3) Deng, R. P.; Herceg, E.; Trenary, M. Characterization of Methylidyne on Pt(111) with Infrared Spectroscopy. *Surf. Sci.* **2004**, *573*, 310−319.
(4) Herceg, E.; Celio, H.; Trenary, M. Sensitivity Improvement in Surface Infrared Spectroscopy: Design, Characteristics, And Application of a High-Temperature Graphite Source. *Rev. Sci. Instrum.* **2004**, *75*, 2545−2550.
(5) Henderson, M. A.; Mitchell, G. E.; White, J. M. The Chemisorption of Methyl Halides (Cl, Br, and I) on Pt(111). *Surf. Sci.* **1987**, *184*, L325−L331.
(6) Henderson, M. A.; Mitchell, G. E.; White, J. M. CH3 and CH3I Chemistry on Pt(111) - The Influence of CO. *Surf. Sci.* **1991**, *248*, 279−286.
(7) Zaera, F.; Hoffmann, H. Detection of Chemisorbed Methyl and Methylene Groups - Surface Chemistry of MethylIodide on Pt(111). *J. Phys. Chem.* **1991**, *95*, 6297−6303.
(8) Hugenschmidt, M. B.; Domagala, M. E.; Campbell, C. T. The Effects of Postdosed Bismuth on the Chemistry of CH3 and CH3I on Pt(111). *Surf. Sci.* **1992**, *275*, 121−130.
(9) French, C.; Harrison, I. Orientation and Decomposition Kinetics of Methyl Iodide on Pt(111). *Surf. Sci.* **1995**, *342*, 85−100.
(10) Panja, C.; Samano, E. C.; Saliba, N. A.; Koel, B. E. Probing the Chemistry of CH3I on Pt-Sn alloys. *Surf. Sci.* **2004**, *553*, 39−49.
(11) Berlowitz, P.; Yang, B. L.; Butt, J. B.; Kung, H. H. Reactions of Azomethane on a Clean, H-Covered and O-Covered Pt(111) Surface. *Surf. Sci.* **1986**, *171*, 69−82.
(12) Fairbrother, D. H.; Peng, X. D.; Viswanathan, R.; Stair, P. C.; Trenary, M.; Fan, J. Carbon Carbon Coupling of Methyl Groups on Pt(111). *Surf. Sci.* **1993**, *285*, L455−L460.
(13) Jentz, D.; Trenary, M.; Peng, X. D.; Stair, P. The Thermal Decomposition of Azomethane on Pt(111). *Surf. Sci.* **1995**, *341*, 282−294.
(14) Fairbrother, D. H.; Peng, X. D.; Trenary, M.; Stair, P. C. Surface Chemistry of Methyl Groups Adsorbed on Pt(111). *J. Chem. Soc., Faraday* **1995**, *91*, 3619−3625.
(15) Zaera, F. Mechanism for the Catalytic Exchange of Methane with Deuterium on Pt(111) Surfaces. *Catal. Lett.* **1991**, *11*, 95−104.
(16) Zaera, F. Study of the Surface Chemistry of Methyl-Iodide Coadsorbed with Hydrogen on Pt(111). *Surf. Sci.* **1992**, *262*, 335−350.
(17) Karp, E. M.; Silbaugh, T. L.; Campbell, C. T. Energetics of Adsorbed CH_3 on Pt(111) by Calorimetry. *J. Am. Chem. Soc.*, in press; DOI: 10.1021/ja400899p.
(18) Lew, W.; Lytken, O.; Farmer, J. A.; Crowe, M. C.; Campbell, C. T. Improved Pyroelectric Detectors for Single Crystal Adsorption Calorimetry from 100 to 350 K. *Rev. Sci. Instrum.* **2010**, *81*, 024102.
(19) Lew, W. D.; Crowe, M. C.; Karp, E.; Campbell, C. T. Energy of Molecularly Adsorbed Water on Clean Pt(111) and Pt(111) with Coadsorbed Oxygen by Calorimetry. *J. Phys. Chem. C* **2011**, *115*, 9164−9170.
(20) Ajo, H. M.; Ihm, H.; Moilanen, D. E.; Campbell, C. T. Calorimeter for Adsorption Energies of Larger Molecules on Single Crystal Surfaces. *Rev. Sci. Instrum.* **2004**, *75*, 4471−4480.
(21) Lytken, O.; Lew, W.; Harris, J. J. W.; Vestergaard, E. K.; Gottfried, J. M.; Campbell, C. T. Energetics of Cyclohexene Adsorption and Reaction on Pt(111) by Low-Temperature Microcalorimetry. *J. Am. Chem. Soc.* **2008**, *130*, 10247−10257.
(22) Stuckless, J. T.; Frei, N. A.; Campbell, C. T. Pyroelectric Detector for Single-Crystal Adsorption Microcalorimetry: Analysis of Pulse Shape and Intensity. *Sens. Actuator B, Chem.* **2000**, *62*, 13−22.
(23) Karp, E. M.; Silbaugh, T. L.; Crowe, M. C.; Campbell, C. T. Energetics of Adsorbed Methanol and Methoxy on Pt(111) by Microcalorimetry. *J. Am. Chem. Soc.* **2012**, *134*, 20388−20395.
(24) King, D. A.; Wells, M. G. Molecular Beam Investigation of Adsorption Kinetics on Bulk Metal Targets - Nitrogen on Tungsten. *Surf. Sci.* **1972**, *29*, 454−482.
(25) Ihm, H.; Ajo, H. M.; Gottfried, J. M.; Bera, P.; Campbell, C. T. Calorimetric Measurement of the Heat of Adsorption of Benzene on Pt(111). *J. Phys. Chem. B* **2004**, *108*, 14627−14633.
(26) Gottfried, J. M.; Vestergaard, E. K.; Bera, P.; Campbell, C. T. Heat of Adsorption of Naphthalene on Pt(111) Measured by Adsorption Calorimetry. *J. Phys. Chem. B* **2006**, *110*, 17539−17545.
(27) Cox, J. D.; Pilcher, G. *Thermochemistry of organic and organometallic compounds*; Academic Press: New York, 1970.
(28) Persson, B. N. J. On the Nature of Adsorbate Phase Diagrams - Beyond the Lattice Gas Models. *Surf. Sci.* **1991**, *258*, 451−463.
(29) Farmer, J. A.; Campbell, C. T. Ceria Maintains Smaller Metal Catalyst Particles by Strong Metal-Support Bonding. *Science* **2010**, *329*, 933−936.
(30) Wren, D. J.; Vikis, A. C. Vapor Pressure of CH3I in the Temperature Range 176 to 227 K. *J. Chem. Thermodyn.* **1982**, *14*, 435−437.
(31) Egan, C. J.; Kemp, J. D. Methyl Bromide - the Heat Capacity, Vapor Pressure, Heats of Transition, Fusion and Vaporization - Entropy and Density of the Gas. *J. Am. Chem. Soc.* **1938**, *60*, 2097−2101.
(32) Paul, A.; Yang, M. X.; Bent, B. E. Disproportionation and Coupling Reactions of Alkyl Iodides on a Au(111) Surface. *Surf. Sci.* **1993**, *297*, 327−344.
(33) Wu, G.; Stacchiola, D.; Collins, M.; Tysoe, W. T. An Infrared-Spectroscopic Study of Methyl Iodide and Methylene Iodide on Ag(111). *Surf. Rev. Lett.* **2001**, *8*, 303−312.
(34) Lin, J. L.; Bent, B. E. 2 Mechanisms for the Formation of Methyl Radicals During the Thermal Decomposition of CH3I on a Cu(111) Surface. *J. Phys. Chem.* **1993**, *97*, 9713−9718.
(35) Lew, W.; Crowe, M. C.; Karp, E.; Lytken, O.; Farmer, J. A.; Arnadottir, L.; Schoenbaum, C.; Campbell, C. T. The Energy of Adsorbed Hydroxyl on Pt(111) by Microcalorimetry. *J. Phys. Chem. C* **2011**, *115*, 11586−11594.
(36) Labayen, M.; Furman, S. A.; Harrington, D. A. A Thermal Desorption Study of Iodine on Pt(111). *Surf. Sci.* **2003**, *525*, 149−158.
(37) Poelsema, B.; Mechtersheimer, G.; Comsa, G. The Interaction of Hydrogen with Platinum(S)-9(111)X(111) Studied with Helium Beam Diffraction. *Surf. Sci.* **1981**, *111*, 519−544.
(38) Donald, S. B.; Harrison, I. Dynamically Biased RRKM Model of Activated Gas-Surface Reactivity: Vibrational Efficacy and Rotation As a Spectator in the Dissociative Chemisorption of CH_4 on Pt(111). *Phys. Chem. Chem. Phys.* **2012**, *14*, 1784−1795.
(39) Chase, M. W. *National Institute of Standards and T. NIST-JANAF thermochemical tables*; American Chemical Society ; American Institute of Physics for the National Institute of Standards and Technology: [Washington, D.C.]; Woodbury, N.Y., 1998.
(40) Yeo, Y. Y.; Stuck, A.; Wartnaby, C. E.; King, D. A. Microcalorimetric Study of Ethylene Adsorption on the Pt{111} Surface. *Chem. Phys. Lett.* **1996**, *259*, 28−36.
(41) Karp, E. M.; Campbell, C. T.; Studt, F.; Abild-Pedersen, F.; Nørskov, J. K. The Energetics of Oxygen Adatoms, Hydroxyl Species and Water Dissociation on Pt(111). *J. Phys. Chem. C* **2012**, *116*, 25772−25776.
(42) Tait, S. L.; Dohnalek, Z.; Campbell, C. T.; Kay, B. D. *n*-alkanes on Pt(111) and on C(0001)/Pt(111): Chain length dependence of kinetic desorption parameters. *J. Chem. Phys.* **2006**, *125*, 234308.

(43) Michaelides, A.; Hu, P. Insight into Microscopic Reaction Pathways in Heterogeneous Catalysis. *J. Am. Chem. Soc.* **2000**, *122*, 9866−9867.
(44) Jacob, T.; Goddard, W. A. Chemisorption of (CHx and C2Hy) Hydrocarbons on Pt(111) Clusters and Surfaces from DFT Studies. *J. Phys. Chem. B* **2005**, *109*, 297−311.
(45) Psofogiannakis, G.; St-Amant, A.; Ternan, M. Methane Oxidation Mechanism on Pt(111): A Cluster Model DFT Study. *J. Phys. Chem. B* **2006**, *110*, 24593−24605.
(46) Kua, J.; Goddard, W. A. Oxidation of Methanol on 2nd and 3rd Row Group VIII Transition Metals (Pt, Ir, Os, Pd, Rh, and Ru): Application to Direct Methanol Fuel Cells. *J. Am. Chem. Soc.* **1999**, *121*, 10928−10941.
(47) Ford, D. C.; Xu, Y.; Mavrikakis, M. Atomic and Molecular Adsorption on Pt(111). *Surf. Sci.* **2005**, *587*, 159−174.
(48) Yang, M. L.; Zhu, Y. A.; Fan, C.; Sui, Z. J.; Chen, D.; Zhou, X. G. Density Functional Study of the Chemisorption of C-1, C-2 and C-3 Intermediates in Propane Dissociation on Pt(111). *J. Mol. Catal. A: Chem.* **2010**, *321*, 42−49.